ARTICLE

Monitoring Polymer Properties Using Shear Horizontal Surface Acoustic Waves

Dana Y. Gallimore,[†,‡] Paul J. Millard,[§,†] and Mauricio Pereira da Cunha*[,†,‡]

Laboratory for Surface Science and Technology, Department of Electrical and Computer Engineering, Department of Chemical and Biological Engineering, University of Maine, Orono, Maine 04469

ABSTRACT Real-time, nondestructive methods for monitoring polymer film properties are increasingly important in the development and fabrication of modern polymer-containing products. Online testing of industrial polymer films during preparation and conditioning is required to minimize material and energy consumption, improve the product quality, increase the production rate, and reduce the number of product rejects. It is well-known that shear horizontal surface acoustic wave (SH-SAW) propagation is sensitive to mass changes as well as to the mechanical properties of attached materials. In this work, the SH-SAW was used to monitor polymer property changes primarily dictated by variations in the viscoelasticity. The viscoelastic properties of a negative photoresist film were monitored throughout the ultraviolet (UV) light-induced polymer cross-linking process using SH-SAW delay line devices. Changes in the polymer film mass and viscoelasticity caused by UV exposure produced variations in the phase velocity and attenuation of the SH-SAW propagating in the structure. Based on measured polymer-coated delay line scattering transmission responses (S_{21}) and the measured polymer layer thickness and density, the viscoelastic constants c_{44} and η_{44} were extracted. The polymer thickness was found to decrease 0.6% during UV curing, while variations in the polymer density were determined to be insignificant. Changes of 6% in c_{44} and 22% in η_{44} during the cross-linking process were observed, showing the sensitivity of the SH-SAW phase velocity and attenuation to changes in the polymer film viscoelasticity. These results indicate the potential for SH-SAW devices as online monitoring sensors for polymer film processing.

KEYWORDS: viscoelasticity monitoring • polymer films • shear horizontal SAW sensor

I. INTRODUCTION

Real-time, nondestructive evaluation (NDE) techniques for polymeric material characterization have important applications in new materials research and industry processes. Polymer films are currently employed as coatings and membranes in industries including textile, biomedical, and paper (1, 2), as waveguiding layers for acoustic-wave sensor devices (3, 4), and as selective layers for chemical sensors (5, 6). Characterization of polymer films during production in real time is desired to minimize material and energy consumption, improve product quality, optimize fabrication protocols, and increase the production rate (7). Changes in polymer film properties such as mass, thickness, and viscoelasticity relate to events such as vapor absorption, solvent evaporation, and polymerization progress.

In particular, properties such as the degree of polymerization and the amount of cross-linking have significant effects on the polymer viscoelasticity but may not affect the mass of the polymer. In these cases, the measurement of the polymer viscoelasticity is desirable to determine the state of a polymer film. Standard methods for measuring the mechanical properties of polymer films, such as differential scanning calorimetry, nanoindentation, and atomic force microscopy (AFM), require specialized equipment, can be expensive and time-consuming, and are not amenable for real-time online process monitoring (2). Acoustic-wave technology, and, in particular, surface acoustic wave (SAW), has the potential for in situ monitoring of polymer films.

Acoustic-wave sensors are used as effective tools for bulk metal and polymer process control measurements (8, 9). Parameters such as mold filling, flow front speed, temperature, and solidification are monitored during injection molding with ultrasonic waves and used to improve the quality and repeatability of the molded parts. These pulse-echo NDE techniques have primarily been used to detect the presence of the polymer within the processing equipment.

Acoustic-wave devices are recognized as sensitive to mass variations, which are directly related to changes in the acoustic-wave velocity (10). Bulk acoustic-wave (BAW) devices have been historically used for mass measurements in the form of quartz crystal microbalances (5, 11, 12). However, recent measurements have shown that acoustic waves are also sensitive to the variations in the mechanical properties of attached layers (13−15). BAW devices have been used to determine the shear modulus of polymer films during temperature changes, vapor sorption, and film drying (16−18). This method was also used to determine the complex shear modulus of polymer films versus the film thickness (19, 20). An approximate method has been used to determine changes in the complex shear modulus of a photoresist polymer during ultraviolet (UV) exposure on an acoustic plate mode device (21). Perturbation theory has

* To whom correspondence should be addressed. E-mail: mdacunha@eece.maine.edu.
Received for review August 3, 2009 and accepted September 17, 2009
† Laboratory for Surface Science and Technology.
‡ Department of Electrical and Computer Engineering.
§ Department of Chemical and Biological Engineering.
DOI: 10.1021/am900512q
© 2009 American Chemical Society

Published on Web 10/01/2009

been used in conjunction with generalized SAW measurements to monitor the polymer properties during temperature changes (22) and to determine the complex shear modulus of a monolayer during a photo-cross-linking reaction (23). Generalized SAW modes have been explored as surface viscosity sensors in liquid and gaseous environments (22−26).

Strong horizontally polarized waves, such as the pseudo-SAWs and certain plate modes, have been used extensively for viscoelastic sensing applications, and pure shear horizontal SAW (SH-SAW) devices have also been explored for physical property measurements. Multiple works have reported pseudo-SAW sensors on $LiTaO_3$ (27, 28) as well as SH-SAW sensors (29, 30) for viscosity measurements. Continuous monitoring of the pseudo-SAW response to polymer vapor deposition has been achieved (31), and the pseudo-SAW response to mass loading and viscoelasticity has been applied to gas sensing (32). The mass sensitivity of polymer-guided pseudo-SAW biosensors has been explored (4), while other works considered the effects of pseudo-SAW and SH-SAW geometry and the polymer-guiding layer thickness on the acoustic-wave sensitivity (33, 34). Perturbation theory has been used in conjunction with pseudo-SAW and SH-SAW measurements to estimate the shear modulus of antibody layers (35, 36), and the sensitivity of the guided SH-SAW response to the DNA length and bending has also been reported (37).

This work investigates the SH-SAW mode for the continuous monitoring of changes in the viscoelastic properties of thin polymer films during polymerization or cross-linking, with potential applications for new materials research and industrial monitoring. In order to design an in situ sensor that is sensitive to the desired film property, it is necessary to understand the relative importance of the mass and viscoelastic properties of films on a sensor platform. The relative effects of mass loading and viscoelasticity along a pure SH-SAW on ST-90° quartz, Euler angles (0°, 132.75°, 90°), are studied using a negative photoresist, which is monitored in real-time throughout the UV polymer curing process. The selected photoresist polymer is not expected to undergo significant changes in thickness or mass as it cross-links but is anticipated to show a more pronounced change in the viscoelasticity. The SH-SAW response, along with independent density and thickness measurements of the film, is used to extract the polymer viscoelastic parameters c_{44} and η_{44}.

Section II of this paper reviews SAW concepts, introduces the polymer film chosen for the work, and explains the viscoelastic constant extraction technique. Section III describes the SH-SAW devices fabricated, the experimental set up, and details of the testing procedure. Section IV presents the results of the work and discusses their significance to online polymer film monitoring. Section V concludes the paper.

II. SH-SAW, SELECTED POLYMER, AND VISCOELASTIC EXTRACTION TECHNIQUE

II.a. SH-SAW. Surface acoustic waves are acoustic waves guided by a substrate surface and are, therefore, particularly sensitive to activity at this boundary. When using SAWs for sensing in liquid and highly viscous media, SH-SAW modes are required because of their diminished attenuation when compared to the generalized SAW, which quickly leaks energy into the surrounding viscous material (38−40). Unlike the generalized SAW and the Rayleigh wave (and, in general, any acoustic wave with significant particle displacement normal to the surface), the SH-SAW mode has particle displacement parallel to the device surface, thus not significantly dissipating acoustic energy into the viscous media. In addition, the SH-SAW phase velocities are usually higher than the generalized SAW phase velocities on a particular crystal cut. Increased phase velocity permits the fabrication of higher frequency devices for the same photolithographic resolution, which also increases the sensor platform sensitivity (41). Furthermore, the small size, quick response time, potential for use in sensor arrays, and portability of the SH-SAW technique are attractive for use in a variety of polymer sensing applications.

This work employs SH-SAW delay line devices, which consist of two interdigitated transducers (IDTs) separated by a metalized delay path. The layer to be measured is applied to the device surface, affecting the phase velocity and attenuation of the SH-SAWs excited and detected by the IDTs. Changes in the phase velocity and attenuation are used to characterize the mechanical properties of the layer.

II.b. Polymer Layer. Negative photoresist ma-N 420 (Micro Resist Technology, Berlin, Germany) is a photolithographic polymer used in the microelectronics industry. All photoresists contain at least two components, a film-forming resin and a solvent system. Most photoresists also contain other additives, such as sensitizers, polymerization inhibitors, and stabilizers (42). Photoresists do not require chemical initiators or temperature change to induce polymer cross-linking and are formulated to cross-link evenly throughout the thickness of the polymer, an important feature for the photolithographic process. The solvents, which allow the polymer to be spun onto surfaces, are removed after spinning by baking the film above the glass transition temperature, T_g. UV light is then applied, which, for negative photoresists such as ma-N 420, cures the exposed polymer regions. In the curing process, adjacent polymer chains form chemical bonds, making the polymer film more resistant to chemical attack or solvation. Depending on the type of photoresist, some molecules may be released from the polymer chains during curing (42).

The properties that make ma-N 420 valuable for semiconductor microfabrication, particularly the ability to cure without a chemical initiator or temperature change, also make the polymer ideal for studying film viscoelastic variations. Because no chemical initiator is required for cross-linking to occur, mass and thickness variations of the film during the curing process are expected to be

minimal. The process of film curing, however, changes the polymer's viscoelasticity because of the different molecular structure of the cross-linked polymer when compared to the un-cross-linked film. Changes in the SH-SAW response due to UV exposure of the film should therefore be dominated by film viscoelasticity variation and not by changes in the film's mass. The ability of the polymer to cross-link at room temperature is also beneficial for SH-SAW measurements to avoid the interference of temperature variations in the extracted values of the phase velocity and attenuation. The SH-SAW ST-90° quartz orientation used in this work has a temperature coefficient of frequency of approximately 1 ppm/°C (43). Finally, the uniformity of the film allows a consistent extraction of the viscoelastic constants using the method described below.

II.c. Viscoelastic Constant Extraction. When a viscoelastic material is deformed by a periodically varying strain, some of the energy is stored and recovered, because of the elastic property of the material, and some of the energy is dissipated as heat, because of the material viscosity (44). Under linear, sinusoidal deformation, the mechanical properties of a viscoelastic material can be specified using abbreviated subscript notation [37] by two 6 × 6 matrices, $\mathbf{C}$ and η, where $\mathbf{C}$ contains the elastic constants and η the viscosity constants (in units of pascals and pascal · seconds, respectively). These two matrices are combined to form the complex viscoelastic constant matrix $\mathbf{C} + j\omega\eta$. The real part relates to energy storage, and the imaginary part relates to energy loss.

The polymer film used in this work is assumed to be lossy and isotropic. The viscoelastic properties of such a material can be described by four independent constants: two elastic constants, c_{11} and c_{44}, and two viscosity constants, η_{11} and η_{44}. The use of the pure SH-SAW mode allows the independent determination of c_{44} and η_{44} (known together as the complex shear modulus) because there is only one component of particle displacement, which is parallel to the surface and perpendicular to the wave propagation direction (38−40).

The response of a polymer film to sinusoidal mechanical deformations in the substrate−layer system is dependent on the excitation frequency, f. At periods ($1/f$) longer than the polymer relaxation time, a polymer behaves as if it were in the rubbery regime. In this regime, all excited polymer movements have time to move from a deformed state back to their original state. At periods shorter than the polymer relaxation time, a polymer behaves as if it were in the glassy regime. In this regime, long-range polymer movements, such as convolutions of the polymer backbone, do not have time to relax from their deformed state back to equilibrium and are essentially frozen in the deformed state (44). Short-range polymer movements, such as atomic vibrations and reptations around chemical bonds, may still occur. In general, for polymers in the glassy regime, c_{44} assumes values of around 10^9 Pa and $\omega\eta_{44} \ll c_{44}$ (25).

The viscoelastic constants are extracted using the matrix method for SAWs (45) oriented along crystal symmetry 4 (46). Wave propagation is arbitrarily chosen to be in the x direction, with the semiinfinite substrate surface lying in the xy plane. A vector $\tau = [\mathbf{T}\ D_z\ \mathbf{v}\ j\omega\varphi]$ containing the variables that must be continuous across the substrate−multilayer interfaces is defined; ω is the radian frequency, $\mathbf{T}$ contains the three normal stress components, D_z is the normal electric displacement, $\mathbf{v}$ contains the three particle velocity components, and $j\omega\varphi$ is the time derivative of the electric potential. The acoustoelectric equations (Hooke's law, the electrical equation of state, Newton's second law, and Gauss's law) are then reduced to a first-order matrix ordinary differential equation (ODE):

$$\frac{d\tau}{dz} = j\omega\mathbf{A}\tau \tag{1}$$

The system matrix, $\mathbf{A}$, is a function of the material constants of a single layer rotated to the desired coordinate system and the phase velocity and attenuation of the SAW. The solution to the ODE can be written as

$$\tau(z+h) = \exp(j\omega\mathbf{A}h) \tag{2}$$

Equation 2 is a transfer matrix that maps τ across a distance h in the z direction. The transfer matrices of the substrate and each layer are sequentially multiplied, thus automatically satisfying the boundary conditions between the different layers. The problem can then be solved by fulfilling the boundary conditions at the top surface and requiring that the fields decay at the semiinfinite substrate. The solution to the boundary condition problem cannot be found analytically, so numerical methods must be applied. In this work, system matrices are formulated using the known constants of the quartz substrate (47) and metallic (gold) delay path layer (48), the polymer film density and thickness, and the SH-SAW phase velocity and attenuation. The film density, thickness, and SH-SAW propagation parameters are experimentally measured. Initial guesses for the unknown parameters, in this case c_{44} and η_{44} of the polymer layer, are input into the matrix method formulation and varied in order to satisfy the boundary conditions discussed above.

For SH-SAW measurements, the polymer film is applied to the entire delay line device surface, including the delay path and IDTs. Because it is desirable to separate the IDT response from the propagation response during extraction of the film constants, a technique has been devised to remove the IDT response using multiple delay lines. In this technique, the scattering transmission (S_{21}) parameters of four delay lines of different lengths are measured and compared. The transmission response, or transfer function, of each delay line can be described in terms of the transfer function of the two IDTs and the transfer function of the delay path

$$S_{21}(f) = F_{IDT}(f)\, F_{DL}(f)\, F_{IDT}(f) \tag{3}$$

where F_{IDT} and F_{DL} are the transfer functions of the IDT and delay path, respectively. Equation 3 can be written in terms of its magnitude and phase as

$$
\begin{aligned}
|S_{21}(f)| &= |F_{\mathrm{IDT}}(f)||F_{\mathrm{DL}}(f)||F_{\mathrm{IDT}}(f)| \\
&= |F_{\mathrm{IDT}}(f)|^2 A(f)\, \mathrm{e}^{\alpha d_{\mathrm{DL}}}
\end{aligned} \tag{4}
$$

$$
\begin{aligned}
\frac{\mathrm{d}\angle S_{21}}{\mathrm{d}f} &= \frac{\mathrm{d}\angle F_{\mathrm{IDT}}(f)}{\mathrm{d}f} + \frac{\mathrm{d}\angle F_{\mathrm{DL}}(f)}{\mathrm{d}f} + \frac{\mathrm{d}\angle F_{\mathrm{IDT}}(f)}{\mathrm{d}f} \\
&= \frac{2\pi d_{\mathrm{IDT}}}{v_{\mathrm{IDT}}} + \frac{2\pi d_{\mathrm{DL}}}{v_{\mathrm{DL}}}
\end{aligned} \tag{5}
$$

where A(f) is a scaling factor of the delay line transfer function, α is the attenuation across the delay path, d_{IDT} and d_{DL} are the lengths of one IDT and the delay path, and v_{IDT} and v_{DL} are the phase velocity across the IDTs and the delay path, respectively. The IDT components, F_{IDT}, d_{IDT}, and v_{IDT}, are identical for all four devices. The attenuation of the SH-SAW can be determined from the derivative of the natural logarithm of eq 4 with respect to d_{DL}, d ln($|S_{21}|$)/dd_{DL}, which is equal to α. The derivative of eq 5 with respect to d_{DL}, $\mathrm{d}^2\angle S_{21}/(\mathrm{d}f\,\mathrm{d}d_{\mathrm{DL}})$, corresponds to $2\pi/v_{\mathrm{DL}}$, from which one can determine the SH-SAW phase velocity across the delay path.

III. DEVICES FABRICATED, EXPERIMENTAL TEST SETUP, AND PROCEDURE

The SH-SAW delay lines were designed with two split-finger IDTs (eight electrodes per wavelength) separated by a gold, metalized propagation path on ST-90° quartz, Euler angles (0°, 132.75°, 90°). The devices were fabricated at the University of Maine clean room facilities using optical photolithography, lift-off patterning techniques, and thin-film e-beam technology to deposit the 150 nm gold layers with 15 nm chromium adhesion layers. Each split-finger IDT has 320 electrodes, an acoustic aperture of 50 wavelengths, an electrode width of 4 μm, and a mark-to-space ratio of 1:1. The delay lines are patterned in sets of four with delay lengths of 3400, 5400, 7400, and 9400 μm, respectively.

A testing system was developed to measure the transmission response of the four delay lines independently while controlling the temperature and humidity. A switching circuit was designed using two GSWA-4-30DR four-way surface mount switches (Mini Circuits, Brooklyn, NY), which allows electronic signals to be applied to each delay line sequentially. The quartz substrate with patterned delay lines was attached with epoxy OE107 (Epoxy Technologies Inc., Billerica, MA) to a PC board that connects to the switching circuit using pin connectors. This fixture allowed the delay line devices to be easily removed from the circuit for multiple photoresist applications. The switching circuit with attached delay lines is shown in Figure 1 together with the removable PC board and SH-SAW delay lines. The electrical connections from the delay lines to the PC board were made with 4 mil platinum wires before application of the photoresist. A Peltier device, Tellurex model CZ1 (Tellurex, Travers City, MI), along with an aluminum heat block and a heat sink, was used to keep the delay lines at 25 ± 0.1 °C, as indicated in Figure 2. To keep the humidity of the system constant, the entire setup was housed in a desiccator during the data collection process. The lid of the desiccator was replaced with a poly(methyl methacrylate) (PMMA) sheet in order to allow the transmission of UV light. The UV transparency of the $^1/_8$ in. PMMA was verified through measurements with a spectrophotometer, Beckman Coulter model DU 640 (Beckman Coulter, Fullerton, CA), with absorption of 0.2 au at 365 nm wavelength. Two 50 Ω coaxial cables were fed into the desiccator from an Agilent 4396B network analyzer (Agilent Technologies, Santa Clara, CA) and attached to the input and output ports of the switching circuit. The complete SH-SAW testing system is shown in Figure 2. Verification of the electrical system operation was achieved by replacing the removable PC board with four short circuits. No significant variations were observed between the different shorted port responses, which indicates the consistent performance of the system for the four different channels. The network analyzer measured the S_{21} transmission response of each device every 2 min. LABVIEW (National Instruments, Austin, TX) was used to control the switching circuit, regulate the device temperature, and collect the S_{21} data from the network analyzer.

The negative photoresist, ma-N 420, was diluted with isopropyl alcohol (1:1 parts per volume) and spun onto the SH-SAW devices, which were already affixed and electrically bonded to the PC board (Figure 1b), at 3500 rpm for 40 s. The spinner was brought to 3500 rpm over 15 s to increase the uniformity of the resulting film. Photoresist dilution was required to decrease the thickness of the polymer film. The

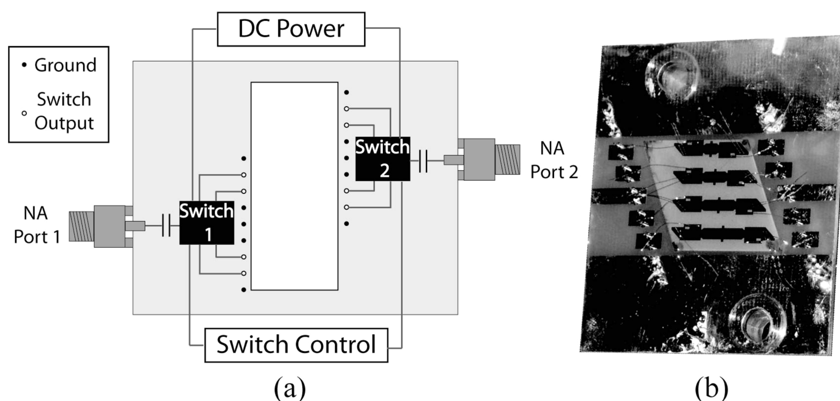

FIGURE 1. (a) Switching circuit. Four-way switches have network analyzer (NA) input and output to the SH-SAW devices via pin connectors. (b) Removable PC board with SH-SAW delay lines attached. The PC board snaps into pin connectors from part a.

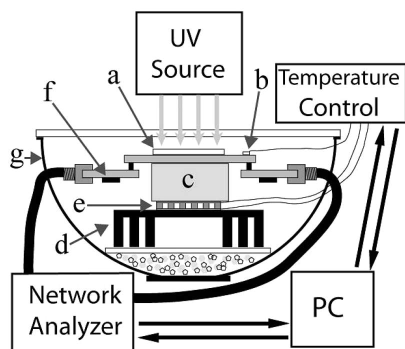

FIGURE 2. Experimental test setup: (a) SH-SAW delay line devices; (b) resistive temperature device; (c) aluminum heat block; (d) heat sink; (e) Peltier device; (f) four-way switch; (g) desiccator.

spun resist was then baked for 1 h at 100 °C to remove solvents. The device was next placed in the described testing system (Figure 2) in the absence of UV light. Once the temperature reached 25 °C (approximately 20 min), UV light was applied to the photoresist using a 100 W mercury lamp with a 330 ± 40 nm filter, and the S_{21} responses of the four delay lines were monitored with the network analyzer over a period of 90 min. The 90 min time frame was determined to be sufficient for complete photoresist curing under the testing conditions during preliminary testing. The inverse fast Fourier transform of the frequency responses obtained were time-gated to minimize interference from wave reflections and unwanted acoustic modes. After the S_{21} responses of the SH-SAW devices with photoresist were measured, a strip of photoresist was removed from the wafer using acetone. The thickness of the exposed photoresist was measured at three locations along the wafer using profilometry.

The viscoelastic properties of very thin polymer films (below ~3% thickness/wavelength) have been shown to be dependent on the film thickness (19, 20). In order to determine the effect of the ma-N 420 thickness on the extracted values of c_{44} and η_{44}, seven polymer films were created using dilution with isopropyl alcohol other than 1:1. These films were measured in the same way as the films previously described, and the thicknesses of the films were measured after UV exposure using profilometry.

For a negative control, photoresist-coated SH-SAW devices (produced with 1:1 photoresist to isopropanol) were prepared in the same manner as previously described. The devices were again placed in the testing system and allowed to reach 25 °C. The S_{21} responses were then measured over a period of 90 min without exposure to UV light.

The density of the polymer film was determined by mass and thickness measurements. Clean quartz wafers were weighed with an Ohaus model AP110 balance (Ohause, Terre Haute, IN), having the repeatability of 0.1 mg. The photoresist was then spun onto the wafers and baked using the procedure described above. The wafers coated with unexposed polymer were weighed, and the mass of the film was found as the difference in weight before and after the application of the film. The photoresist was then exposed, and the mass was measured again, in an attempt to determine any significant change in mass due to photoresist exposure. The volume of the film was determined from the surface area of the quartz wafers and the thickness of the polymer film as measured by profilometry. The density of the film was calculated from the calculated volume and the measured mass after exposure.

Profilometry was useful in estimating the photoresist thickness but was not suitable for measuring the small changes in thickness caused by photoresist exposure. Profilometry measurements proved to be nonrepeatable and inadequate to deliver a reliable reading because of (i) the poorly defined step produced by removal of the photoresist with acetone and (ii) the typical variations in the photoresist thickness that occur across the polymer surface. Ellipsometry was used to determine any eventual variation in the photoresist thickness before and after UV exposure because this technique did not require photoresist removal. However, ellipsometry could not be performed on the delay line devices directly because of the gold-patterned quartz surface. Therefore, the photoresist was applied to nonmetalized quartz wafers and baked as previously described. Ellipsometry measurements were then performed on the polymer film before and after exposure to UV light (49). The polymer layer thickness was determined by fitting the measured data to a Cauchy layer model (50). These thickness values were compared in order to calculate the change in the film thickness caused by UV-light exposure.

In addition to density estimation from mass and volume data, X-ray reflectivity (XRR) measurements were performed to investigate density changes in the photoresist caused by exposure to UV light (51). Photoresist-coated quartz wafers were prepared as for the ellipsometry measurements. The XRR measurements were then taken before and after exposure of UV light to the photoresist. The change in the density was determined from the measured critical angles of the unexposed and exposed films.

IV. RESULTS AND DISCUSSION

Five polymer samples were identically prepared on the SH-SAW devices using 1:1 dilution with isopropyl alcohol as described in section III. The mean thickness of the UV-exposed polymer films, as measured by profilometry, was 1.23 μm with a standard deviation of 50 nm across the five wafers. For the five samples, mean changes in the phase velocity and attenuation of the SH-SAWs due to UV exposure of the polymer were 3% and 11%, respectively. For the control samples, which were not exposed to UV light, the measured change in the phase velocity, v_p, was less than 0.3% and the measured change in the attenuation, α, was 1.5%, which may have been caused by solvent evaporation or minimal UV-light exposure. These results ensure that measured changes in the phase velocity and attenuation are predominantly UV-light-induced. Figure 3 shows the v_p/v_0 and α/α_0 vs time responses of one of the identically prepared ma-N 420 films, where v_0 and α_0 are the velocity and attenuation at 0 min. The measured exposed thickness, h, of this particular sample was 1.14 μm. The control measurements are included in Figure 3 for comparison.

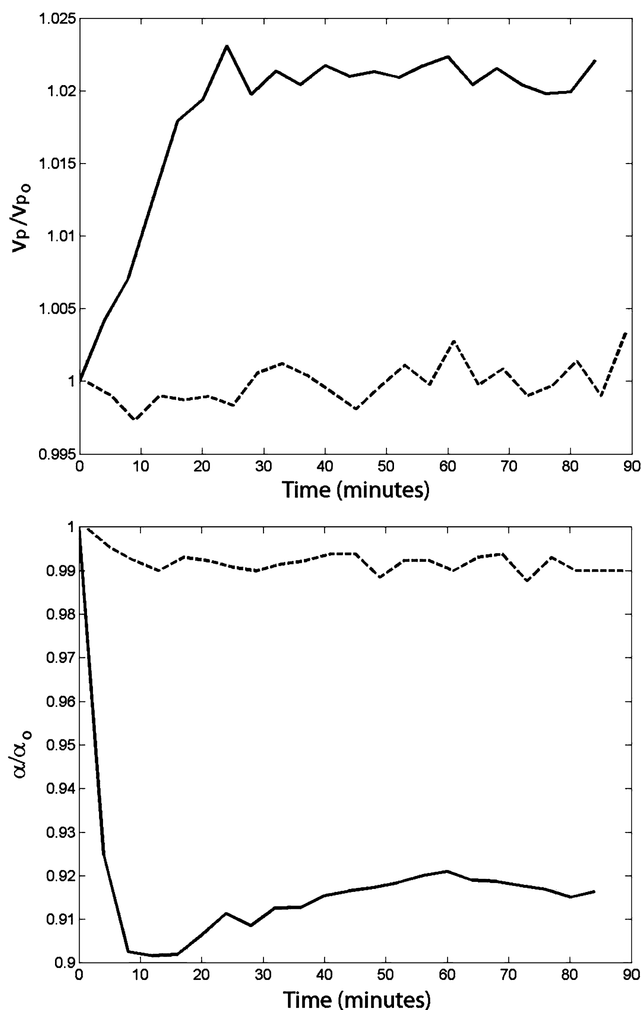

FIGURE 3. Measured v_p/v_0 and α/α_0 vs UV exposure time for the $h = 1.14\ \mu$m, 1:1 diluted photoresist sample. The solid line indicates the test sample; the dotted line indicates the control sample (no UV light was applied).

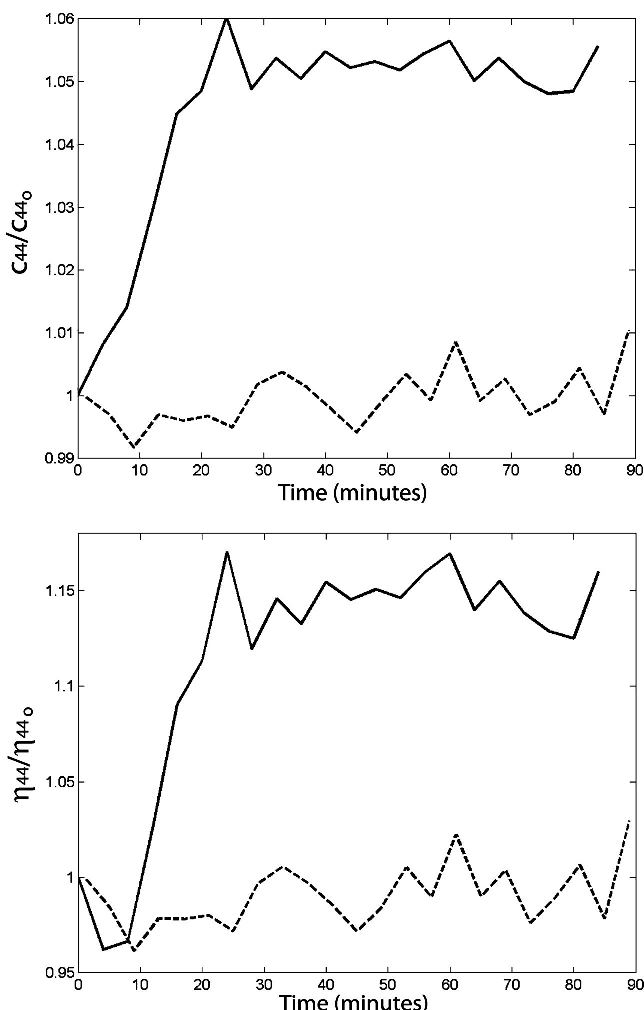

FIGURE 4. Extracted values of $c_{44}/c_{44,0}$ and $\eta_{44}/\eta_{44,0}$ vs UV exposure time for the $h = 1.14\ \mu$m sample shown in Figure 3. The solid line denotes the test sample; the dotted line indicates the control sample.

In order to translate the variations in v_p/v_0 and α/α_0 vs time into viscoelastic variations, the film density is required. As discussed in the previous section, the film density was obtained by measuring the mass of a 1:1 diluted polymer film spread over quartz wafers with a surface area of 45.4 $\pm$ 0.2 cm^2. In order to increase the value of the polymer film mass to be extracted, two quartz wafers with 1:1 diluted photoresist were jointly measured and resulted in a polymer mass of 14.8 $\pm$ 0.1 mg. The polymer film thicknesses for the two wafers were measured using the profilometer and added, resulting in 2.26 $\pm$ 56 nm. The uncertainty in the thickness measurement was determined based on the waviness of the polymer surface, which is 40 nm for each of the samples measured. From the area of both wafers and the combined mass and thickness, the density was calculated to be 1.44 $\pm$ 0.04 g/cm^3.

In order to verify potential thickness and density variations before and after UV exposure, ellipsometry, mass measurements, and XRR techniques were used. Ellipsometry showed an average decrease in the film thickness of 0.62% with a standard deviation of 0.53% due to UV-light exposure. The mass change due to photoresist exposure was smaller than the 0.1 mg limit of the balance used, which translates to a mass variation of smaller than 0.7% and therefore a density variation of less than 0.1%. This result is consistent with the XRR measurements, which indicated that the photoresist density variation due to UV-light exposure is within the $\pm$0.4% limit of the measurement system. Any changes in density were therefore small and below the instrumentation capabilities. This behavior was expected for the ma-N 420 polymer because glassy polymers contract or expand to retain a constant density when molecules are lost or added (21). Because of the negligible variations identified above, the density was assumed to remain constant.

The viscoelastic constants for each of the five 1:1 diluted polymer films were extracted as a function of the exposure time using the measured phase velocity and attenuation data along with the exposed film thickness value obtained from profilometry, the 0.62% decrease in thickness measured by ellipsometry, and the extracted 1.44 g/cm^3 density value. These data were input into the matrix method formulation as described in section II for each measurement instance. Because the 0.62% thickness decrease was not continuously monitored during UV exposure, its functional dependence

Table 1. Mean Values for v_p, α, c_{44}, and η_{44} before and after Photoresist Exposure[a]

$\bar{v}_{p,0}$ (m/s)	$\Delta\bar{v}_p$ (m/s)	$\bar{\alpha}_0$ (dB/λ)	$\Delta\bar{\alpha}$ (dB/λ)	$\bar{c}_{44,0}$ (GPa)	$\Delta\bar{c}_{44}$ (GPa)	$\bar{\eta}_{44,0}$ (mPa·s)	$\Delta\bar{\eta}_{44}$ (mPa·s)	$\bar{h}$ (μm)
3513 ± 351	105 ± 45	0.105 ± 0.038	0.012 ± 0.005	0.50 ± 0.04	0.03 ± 0.01	0.79 ± 0.33	0.17 ± 0.04	1.23 ± 0.05

[a] Listed uncertainty values reflect the standard deviation of measurements between the five polymer samples.

with time was assumed to be exponential. Figure 4 shows normalized $c_{44}/c_{44,0}$ and $\eta_{44}/\eta_{44,0}$ vs time for the control sample and the UV-exposed $h = 1.14$ μm sample, with $c_{44,0}$ and $\eta_{44,0}$ being the values for c_{44} and η_{44} at 0 min. A mean change of 6% in c_{44} and 22% in η_{44} vs exposure time was extracted for the five samples measured. The mean collected data for the 1:1 diluted films regarding the phase velocity, attenuation, stiffness, viscosity, and respective variations before and after UV exposure are listed in Table 1. The listed uncertainty values reflect the standard deviation of measured data between the five samples. From the extracted viscoelastic constants and the SH-SAW frequency, the polymer is in the glassy regime ($\omega\eta \ll c$; $\omega = 3\pi \times 10^8$ rad/s) with mean elastic constant values of 0.5018 and 0.5319 GPa before and after it is cured, respectively.

The standard deviations of the measured SH-SAWs' phase velocity and attenuation across the five 1:1 diluted polymer-coated delay lines before polymer curing were 10% and 36%, respectively. This spread in the results for the identically prepared polymer indicated that variations in the thickness have a significant effect on the SH-SAW propagation properties, which is a positive effect in a thickness monitoring sensor application. In order to verify the influence of the film thickness in the measured values of the phase velocity and attenuation and therefore the viscoelastic properties extracted, ma-N 420 films from 230 nm to 1.2 μm were measured. A 1:9 photoresist dilution in isopropyl alcohol resulted in the 230 nm film thickness and was adopted as the upper dilution limit for this test. The 1:1 dilution, which resulted in a 1.2 μm thick film, was adopted as the lower dilution limit. Undiluted photoresist resulted in films with thicknesses of around 2 μm and excessive SH-SAW transmission loss (>30 dB) on the ST-90° quartz orientation as a result of viscoelastic attenuation and possible mode conversion. It is worth noting, however, that the film thickness limit depends on the substrate, orientation, and viscoelastic properties of the layer. Different substrates, orientations, and polymer types result in different upper thickness limits.

Figure 5 shows the extracted values of c_{44} and η_{44} vs thickness after exposure. The sixth data point (denoted by an "×" in the figure) represents the $h = 1.14$ μm sample shown in Figures 3 and 4. As can be observed from Figure 5, the viscoelastic constants indeed have a strong dependence on the thin-film thickness. This dependence explains the variation of the phase velocity and attenuation values measured for the 1:1 diluted films. This identified sensitivity to the film thickness is a positive feature for sensor applications because the SH-SAW method can be tailored to monitor the film mechanical and/or thickness properties through extraction of the viscoelastic constants.

In order to be a useful tool for monitoring the mechanical properties of polymer films, the SH-SAW device must be sufficiently sensitive to changes in the viscoelastic parameters. The sensitivity of the SH-SAW phase velocity and attenuation responses to variations in the viscoelastic constants was determined by calculating the incremental variations in v_p and α from the incremental variations in c_{44} and η_{44}. These sensitivity coefficients are listed in Table 2. The extracted c_{44} and η_{44} were used to calculate the phase velocity and attenuation for a fixed thickness (the uncured polymer thickness) and density and compared to the mea-

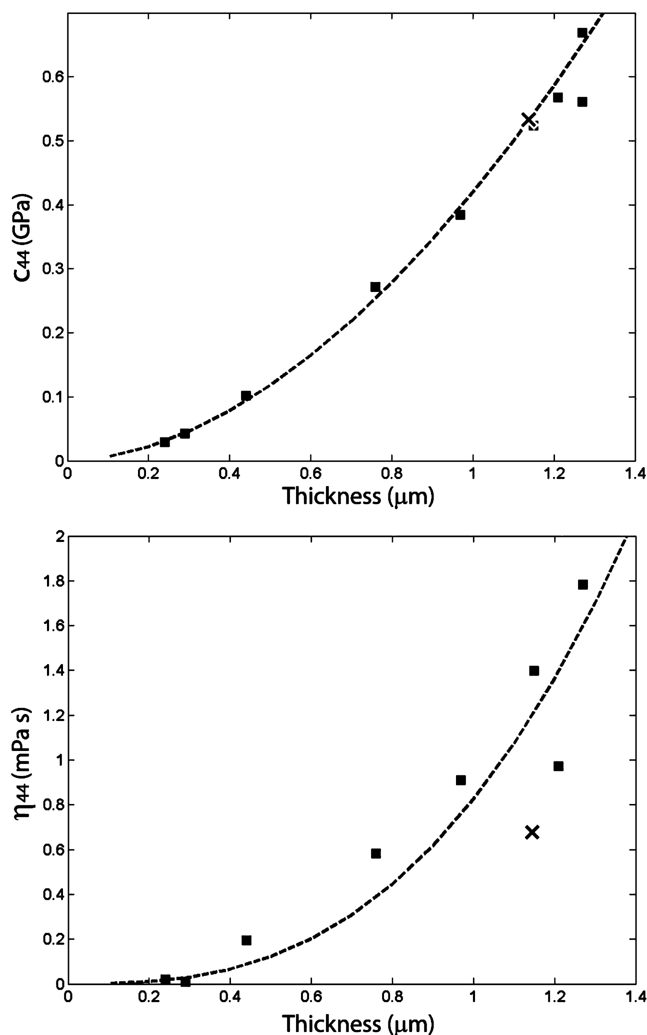

FIGURE 5. Extracted values of c_{44} and η_{44} vs photoresist thickness after UV exposure. Squares indicate extracted points, × indicates extracted values for the $h = 1.14$ μm sample shown Figures 3 and 4, and the dotted line indicates the best-fit curve.

Table 2. Sensitivity of the SH-SAW Phase Velocity and Attenuation Responses to Changes in the Elasticity (c_{44}) and Viscosity (η_{44}) of the Polymer Coating

$\Delta v_p/\Delta c_{44}$ (m/s/GPa)	$\Delta v_p/\Delta\eta_{44}$ (m/s/mPa·s)	$\Delta\alpha/\Delta c_{44}$ (dB/λ/GPa)	$\Delta\alpha/\Delta\eta_{44}$ (dB/λ/mPa·s)
3187	183	0.1230	0.0053

sured values of v_p and α. This analysis showed that the contributions of c_{44} and η_{44} variations to the measured v_p and α changes of the 1:1 diluted samples during UV exposure were 73% and 62%, respectively. Assuming measurement resolutions of 0.5 m/s for the phase velocity and 0.05 dB for the attenuation typical of a network analyzer, one can measure changes as small as 1.5×10^{-4} GPa in c_{44} and 3×10^{-2}mPa·s in η_{44}.

The SH-SAW sensitivity to multiple film parameters, such as elasticity, viscosity, and thickness examined in this work, indicates that this technique can be tailored to identify and quantify particular events of interest during film formation and processing. The SH-SAW devices detected changes in the phase velocity and attenuation due to photoresist cross-linking, which translated into measurable changes in the polymer viscoelasticity. The reported SH-SAW technique is therefore sufficiently sensitive to monitor online changes in the polymer viscoelasticity, with application in new materials research and polymer film production.

V. CONCLUSIONS

This work reported on the viscoelastic response of SH-SAW devices to monitor the cross-linking of polymers in real time, with immediate applications in polymer film development and process control. The viscoelastic constants of a photoresist polymer were extracted throughout UV-light exposure using the matrix method for pure SH-SAWs. Changes of 6% in c_{44} and 22% in η_{44} were observed during the cross-linking process. Sensitivities of the phase velocity and attenuation of SH-SAWs to changes in the elasticity and viscosity were determined for a range of measurable film thicknesses of the chosen polymer. Because of the small size, quick response time, and sensitivity to thickness and viscoelastic constants of the SH-SAW devices, these devices and the methodology described in this work were successfully employed to measure the polymer properties in situ with attractive features regarding existing sensors and technology. On the basis of the results obtained, the SH-SAW method for polymer film monitoring described is a potential candidate for use in industrial settings to improve the quality and consistency of manufactured polymer layers and also to reduce the time, energy, and materials required to fabricate or deposit polymer films.

REFERENCES AND NOTES

(1) Castelvetro, V.; Ciardelli, F.; Francini, G.; Baglioni, P. *Macromol. Mater. Eng.* **2000**, *278*, 6–16.
(2) Fried, J. R. *Polymer Science and Technology*; Prentice Hall: Upper Saddle River, NJ, 2003.
(3) Gizeli, E.; Goddard, N. J.; Stevenson, A. C.; Lowe, C. R. *Sens. Actuators, B* **1992**, *6*, 131–137.
(4) Josse, F.; Bender, F.; Cernosek, R. *Anal. Chem.* **2001**, *73*, 5937–5944.
(5) King, W. H. *Anal. Chem.* **1964**, *36*, 1735–1739.
(6) Patel, R.; Zhou, R.; Zinszer, K.; Josse, F. *Anal. Chem.* **2000**, *72*, 4888–4898.
(7) Featherstone, A. P.; Braatz, R. D. *Proc. Am. Control Conf.* **1995**, 2692–2696.
(8) Jen, C. K.; Liaw, J. W.; Chen, T. F.; Mareau, A.; Monchalin, J. P.; Yang, C. C. *Meas. Sci. Technol.* **2000**, *11*, 1570–1575.
(9) Franca, D. R.; Wen, S.; Jen, C. K.; Nguyen, K. T.; Hebert, H. *Proc. IEEE Ultrason. Symp.* 2000.
(10) Sauerbrey, G. *Z. Physik.* **1959**, *155*, 206.
(11) Oberg, P.; Lingensjo, J. *Rev. Sci. Instrum.* **1959**, *30*, 1053.
(12) O'Sullivan, C. K.; Guilbault, G. G. *Biosens. Bioelectron.* **1999**, *14*, 663–670.
(13) Grate, J. W.; Klusty, M.; McGill, R. A.; Abraham, M. H.; Whiting, G.; Andonian-Haftvan, J. *Anal. Chem.* **1992**, *64*, 610–624.
(14) Liron, Z.; Kaushansky, N.; Frishman, G.; Kaplan, D.; Greenblatt, J. *Anal. Chem.* **1997**, *69*, 2848–2854.
(15) Rickert, J.; Gopel, W.; Hayward, G. L.; Cavic, B. A.; Thompson, M. In *Sensors Update*; Baltes, H., Gopel, W., Hesse, J., Eds.; Wiley VCH: Weinheim, Germany, 1999; Vol. 5, pp 105–139.
(16) Lucklum, R.; Behling, C.; Cernosek, R. W.; Martin, S. J. *J. Phys. D: Appl. Phys.* **1997**, *30*, 346–356.
(17) Behling, C.; Lucklum, R.; Hauptmann, P. *Meas. Sci. Technol.* **1998**, *9*, 1886–1893.
(18) Katz, A.; Ward, M. D. *J. Appl. Phys.* **1996**, *80*, 4153–4163.
(19) Hossenlopp, J.; Jiang, L.; Cernosek, R.; Josse, F. *J. Polym. Sci., Part B: Polym. Phys.* **2004**, *42*, 2373–2384.
(20) Morray, B.; Li, S.; Hossenlopp, J.; Cernosek, R. W.; Josse, F. *Proc. IEEE Freq. Control Symp.* **2002**, 294–300.
(21) Martin, S. J.; Ricco, A. J. *Sens. Actuators* **1990**, *A21-A23*, 712–718.
(22) Ballantine, D. S.; Wohltjen, H. *Proc. IEEE Ultrason. Symp.* **1988**, 559–562.
(23) Ricco, A. J.; Staton, A. W.; Crooks, R. M.; Kim, T. *Faraday Discuss.* **1997**, *107*, 247–258.
(24) Martin, S. J.; Frye, G. C. *Appl. Phys. Lett.* **1990**, *57*, 1867–1869.
(25) Martin, S. J.; Frye, G. C. *Anal. Chem.* **1994**, *66*, 2201–2219.
(26) Kikuchi, T.; Moriizumi, T. *Jpn. J. Appl. Phys.* **1986**, *25*, 43–45.
(27) Nomura, T.; Saitoh, A.; Horikoshi, Y. *Sens. Actuators, B* **2001**, *76*, 69–73.
(28) Kondoh, J.; Hayashi, S.; Shiokawa, S. *Jpn. J. Appl. Phys.* **2001**, *40*, 3713–3717.
(29) Jakoby, B.; Vellekoop, M. J. *Sens. Actuators, A* **1998**, *68*, 275–281.
(30) Josse, F.; Shana, Z. *J. Acoust. Soc. Am.* **1988**, *84*, 978–984.
(31) Bender, F.; Lange, K.; Barie, N.; Kondoh, J.; Rapp, M. *Langmuir* **2004**, *20*, 2315–2319.
(32) Jones, Y. K.; Li, Z.; Johnson, M. M.; Josse, F.; Hossenlopp, J. *IEEE Sens. J.* **2005**, *5*, 1175–1184.
(33) Gizeli, E.; Bender, F.; Rasmusson, A.; Saha, K.; Josse, F.; Cernosek, R. W. *Biosens. Bioelectron.* **2003**, *18*, 1399–1406.
(34) Li, Z.; Jones, Y.; Hossenlopp, J.; Cernosek, R. W.; Josse, F. *Anal. Chem.* **2005**, *77*, 4595–4603.
(35) Weiss, M.; Welsch, W.; Schickfus, M. v.; Hunklinger, S. *Anal. Chem.* **1998**, *70*, 2881–2887.
(36) Saha, K.; Bender, F.; Rasmusson, A.; Gizeli, E. *Langmuir* **2003**, *19*, 1304–1311.
(37) Tsortos, A.; Papadakis, G.; Mitsakakis, K.; Melzak, K. A.; Gizeli, E. *Biophys. J.* **2008**, *94*, 2706–2715.
(38) Pereira da Cunha, M.; Malocha, D. C.; Puccio, D. W.; Thiele, J.; Pollard, T. B. *IEEE Sens. J.* **2003**, *3*, 554–561.
(39) Pereira da Cunha, M.; Malocha, D. C.; Puccio, D. W.; Thiele, J.; Pollard, T. B. *Proc. IEEE Ultrason. Symp.* **2002**, 381–384.
(40) Andle, J. C.; Vetelino, J. F. *Proc. IEEE Ultrason. Symp.* **1995**, 451–460.
(41) Kovacs, G.; Venema, A. *Appl. Phys. Lett.* **1992**, *61*, 639–641.
(42) DeForest, W. *Photoresist*; McGraw-Hill: New York, 1975.
(43) Kadota, M.; Yoneda, T.; Fujimoto, K.; Nakao, T.; Takata, E. *Jpn. J. Appl. Phys.* **2001**, *40*, 3718–3721.
(44) Ferry, J. D. *Viscoelastic Properties of Polymers*; John Wiley & Sons: New York, 1980.
(45) Adler, E. L. *IEEE Trans. Ultrason., Ferroelect., Freq. Control* **1990**, *37*, 485–490.
(46) Farnell, G. W.; Adler, E. L. In *Physical Acoustics Principles and Methods*; Mason, W. P., Thurston, R. N., Eds.; Academic Press: New York, 1972; Vol. 9, pp 35–87.
(47) Bechmann, R. *Phys. Rev.* **1958**, *110*, 1060–1061.
(48) Anderson, O. L.; Isaak, D. G.; Yamamoto, S. *J. Appl. Phys.* **1989**, *65*, 1534–1543.
(49) Korte, E. H.; Roseler, A. *Analyst* **1998**, *123*, 647–651.
(50) *Guide to Using WVASE32*; J. A. Woollam Co., Inc.: Lincoln, NE, 1995.
(51) Birkholz, M. *Thin Film Analysis by X-Ray Scattering*; Wiley-VCH: Weinheim, Germany, 2006.

AM900512Q